变电站接地网的焊缝腐蚀分析

冯拉俊[1]， 邓 博[1]， 闫爱军[2]， 张 静[1]
(1. 西安理工大学 陕西省腐蚀与防护重点实验室，西安 710048; 2. 陕西电力科学研究院，西安 710054)

摘 要: 为了给接地网焊缝的腐蚀防护提供基础，通过电化学噪声和埋片模拟方法，研究了接地网焊缝与母材腐蚀的差别. 结果发现在陕西省孝义变电站土壤中，Q235 钢接地网焊缝出现了较多暂态峰，母材的暂态峰较少，焊缝腐蚀对接地网泄流的电压更敏感; 腐蚀过程中母材噪声阻值 $R_n = 3.38 \times 10^4\ \Omega/cm^2$，焊缝噪声阻值 $R_n = 1.44 \times 10^4\ \Omega/cm^2$; 母材的腐蚀速率为 0.067 mm/a，含有焊缝的焊接接头腐蚀速率为 0.077 mm/a，母材为均匀腐蚀，焊缝主要为局部腐蚀.

关键词: 接地网; 焊缝腐蚀; 电化学噪声; 局部腐蚀
中图分类号: TG 171 **文献标识码**: A **文章编号**: 0253 - 360X(2014) 10 - 0069 - 04

0 序 言

电力接地网是关系电力设备安全运行的关键设备之一[1]. 大多数接地网是由普通碳钢焊接而成，长期埋于地下经受土壤的电化学腐蚀[2,3]及运行设备泄漏电流等造成的杂散电流腐蚀[4,5]，接地网多则10年，少则3～4年便发生损坏甚至断裂. 为此人们对接地网的腐蚀与防护进行了多方面的研究，但对接地网的焊缝腐蚀研究的较少，对其腐蚀的规律还没有掌握，便有两种腐蚀的观点，一种认为焊接接头发生较快腐蚀[6]，引起接地网腐蚀破坏; 另一种认为在土壤中焊接接头不存在比接地网更严重的腐蚀，不需要对焊接接头进行防腐，为此国家电网公司专列课题进行攻关研究，文中研究作为其中的一部分，主要目的是研究接地网焊缝与母材的腐蚀差别，为接地网的焊接方法选择、焊接接头的防护提供理论依据. 为了较快地发现焊接接头与母材的腐蚀差别，研究过程采用电化学噪声和静态埋片方法探索了接地网焊接接头的腐蚀规律.

1 试验方法

文中采用的土壤为渭南孝义750 kV变电站的土壤，接地网材料为目前变电站采用的Q235普通碳钢. 对60 mm×6 mm的Q235普通扁钢，打磨为30°的坡口，采用变电站施工中使用的焊条电弧焊对焊，所用焊条为J422. 将焊接接头和母材制成50 mm×25 mm×3 mm的试样，保证焊缝在试样的中间位置. 对制备的试样先在磨床上磨平，然后采用砂纸逐级打磨，一直打磨到500号砂纸，使表面明亮无划痕后再用丙酮清洗.

将研究试样埋入地下0.8 m深土壤中，在试样表面附近接参比电极，参比电极为饱和氯化钾甘汞电极，在地下0.2 m处接同材质辅助电极. 测试仪器为CS350电化学工作站.

2 试验结果及分析重建算法

2.1 电化学噪声研究结果及分析

对Q235钢接地网在土壤中测试的母材和焊缝的电流和电压噪声谱如图1所示. 从图1可以看出，母材和焊缝试样的电流噪声谱和电压噪声谱都包含了许多暂态峰，暂态峰变化与土壤腐蚀过程中电极表面亚稳态蚀点的萌发和消亡过程有关[7,8]，暂态峰越多，说明腐蚀为局部腐蚀，且局部腐蚀越厉害. 对比图1中母材和焊缝的噪声图谱发现，焊缝试样电流和电压的噪声比母材的都大，特别是母材的电压噪声特别小，而焊缝的电压噪声特别大，这说明母材在土壤中基本为均匀腐蚀，焊缝发生了局部腐蚀，焊缝的腐蚀对电位更敏感.

噪声特征可以用功率谱密度 ρ_{PSD} 来表示，电位或电流的时域信号通过直流漂移处理后经快速傅立叶变换(FFT)可变换成 ρ_{PSD}，并得到功率谱密度与频率的曲线，由此曲线可进行腐蚀极化的阻值分析[9]. ρ_{PSD} 描述的是信号或者时间序列的能量如何随着频

收稿日期: 2013 - 03 - 20
基金项目: 国家电网公司科技资助项目(5226KY11003300); 陕西省教育厅重点实验室资助项目(13JS077)

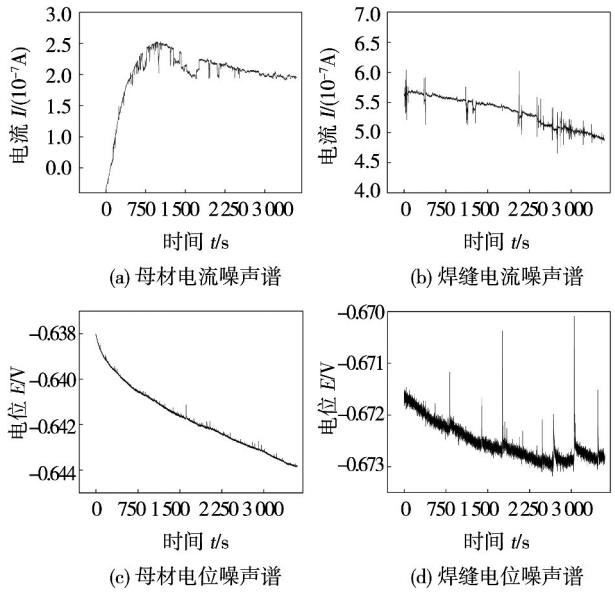

图 1 母材和焊缝噪声谱图

Fig. 1 Noise current and potential time series for Q235 base metal and weld metal

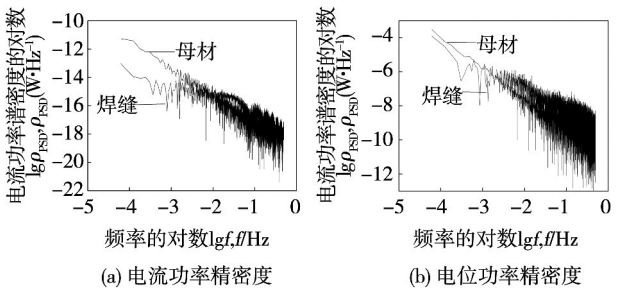

图 2 母材和焊缝电化学噪声信号的 PSD 图

Fig. 2 Potential and current power spectral density plots for Q235 base metal and weld joint

率变化，如果 $f(t)$ 是一个有限能量信号，其平方可积，信号谱密度 $\Phi(\omega)$ 是能量信号 $f(t)$ 连续傅里叶变换幅度的平方，则 $\Phi(\omega)$ 的函数形式为[10,11]

$$\Phi(\omega) = \left|\frac{1}{\sqrt{2\pi}}\int_{+\infty}^{-\infty} f(t)\,\mathrm{e}^{-i\omega t}\mathrm{d}t\right|^2 = \frac{F(\omega)\,F^*(\omega)}{2\pi} \tag{1}$$

式中：ω 为角频率(循环频率的 2π 倍)；t 为时间；$F(\omega)$ 为 $f(t)$ 的连续傅里叶变换. $F^*(\omega)$ 是 $F(\omega)$ 的共轭函数. 图 1 中电位(E)或电流(I)信号经以上 FFT 处理后得到频域谱即功率谱密度图，如图 2 所示.

利用 ENTools 软件对图 2 中母材和焊缝的功率谱密度进行特征频率 f_c 计算[12]，得出母材和焊缝功率谱密度曲线上的特征频率 f_c 分别为 0.391 5 Hz 和 0.448 0 Hz，比较得出在相同测试条件下，母材的 f_c 较小，说明在土壤中母材比焊缝更不容易腐蚀.

利用 Eden[11,13] 提出的噪声电阻

$$R_n = \frac{S_V}{S_i} \tag{2}$$

式中：S_V 和 S_i 分别为噪声电位和噪声电流标准差. Gouveia 等人[14] 认为 R_n 与极化电阻具有一致性，Chen 等人[15]. 进一步指出噪声电阻等效于极化电阻. 因此电极腐蚀速率越大，土壤中电阻的极化越小，即 R_n 越小. 通过对图 1 中母材和焊缝电位和电流噪声谱进行计算，得出如表 1 所示噪声谱参数. 由表 1 可以看出，母材 $R_n = 3.38 \times 10^4\ \Omega/\mathrm{cm}^2$，焊缝 $R_n = 1.44 \times 10^4\ \Omega/\mathrm{cm}^2$，说明在相同土壤中，Q235 钢母材的腐蚀速率要小于焊缝.

表 1 噪声谱计算参数

Table 1 Calculating parameter of EN maps

试样	电压标准差 $S_V/(10^{-3})$	电流标准差 $S_i/(10^{-8})$	电流均方根 $I_{RMS}/(10^{-7}\ \mathrm{A})$	噪声电阻 $R_n/(10^4\ \Omega\cdot\mathrm{cm}^{-2})$	点蚀指标 N
母材	1.40	4.13	5.35	3.38	0.077 31
焊缝	0.364	2.52	2.05	1.44	0.122 69

2.2 埋片腐蚀研究结果及分析

试验土壤的理化性质见表 2. 将含有焊缝的试样和母材同时埋入土壤中，试验周期为两个月，以试验前后试样的质量损失计算其腐蚀速率，测试的腐蚀结果为：母材的腐蚀速率为 0.067 mm/a，含有焊缝试样的腐蚀速率为 0.077 mm/a.

表 2 试验土壤的理化性质

Table 2 Physical and chemical properties of soil used in this experiment

含水量 $W(\%)$	离子含量 $W_R/(\mathrm{mmol}\cdot\mathrm{kg}^{-1})$		酸度 $A_c/(\mathrm{mmol}\cdot\mathrm{kg}^{-1})$	碱度 $B_a/(\mathrm{mmol}\cdot\mathrm{kg}^{-1})$	含盐量 $w_{TDS}/(\mathrm{mg}\cdot\mathrm{kg}^{-1})$	pH
	SO_4^{2-}	Cl^-				
25	8	90	20	600	3 000	8

由现场腐蚀埋片试验结果可见,焊接接头试样腐蚀速度明显大于母材,由绝对值看,好像腐蚀速率相差不大,但焊接接头试样的尺寸为 50 mm × 25 mm × 3 mm,焊缝只有约 4 mm 宽,25 mm 长,相对焊接接头试样,焊缝的面积是非常小的,当把焊接接头试样比母材试样腐蚀速率的增大值认为由焊缝腐蚀引起,由于焊缝面积较小,则焊缝的腐蚀比母材大得多. 焊接接头试样和母材试样的腐蚀宏观形貌见图 3. 由图 3 可见,母材表面虽然有均匀的腐蚀小坑,但整个表面基本还是光亮的,在焊接接头试样的焊缝处,表面已经完全腐蚀,腐蚀的坑比母材大得多.

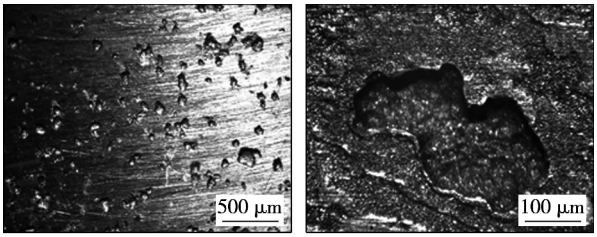

(a) 母材　　(b)焊缝

图 3　焊接接头试样和母材试样的腐蚀宏观形貌

Fig. 3　Macrophotograph of Q235 weld joint and base metal after corrosion

为了进一步分析焊缝在土壤中的腐蚀速度快的原因,对两种材料的组织进行了金相分析,见图 4. 由图 4a 可见,母材的显微组织为晶粒细小均匀的等轴晶,具有良好的耐蚀性. 由图 4b 可见,焊缝显微组织中存在大量的针状铁素体以及珠光体,即魏氏体组织,这种组织的特点是粗大针状铁素体中包含有伪珠光体组分,从而降低了其焊缝的耐蚀性[16,17].

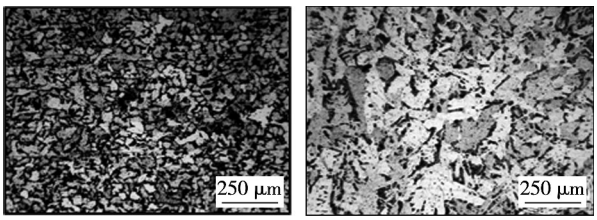

(a) 母材　　(b)焊缝

图 4　母材和焊缝显微组织

Fig. 4　Metallograph for Q235 base metal and weld metal

3　结　　论

(1) 由 Q235 钢接地网在土壤中母材和焊缝的电流和电压噪声谱得到,焊缝出现了较多暂态峰,母材的暂态峰较少,母材主要为均匀腐蚀,焊缝发生了局部腐蚀; 接地网的焊缝腐蚀对电压更敏感; 腐蚀过程母材噪声阻值为 $3.38 \times 10^4\ \Omega/cm^2$,焊缝噪声阻值为 $1.44 \times 10^4\ \Omega/cm^2$.

(2) 在陕西省孝义变电站土壤中,母材的腐蚀速率为 0.067 mm/a,焊接接头腐蚀速率为 0.077 mm/a. 光学显微镜观察腐蚀形貌为母材表面形成均匀的小蚀坑,而焊缝处形成较大的腐蚀坑.

(3) 焊缝与母材的组织不同,母材的组织主要为细小均匀的等轴晶,焊缝组织中存在大量的针状铁素体以及珠光体组织,即魏氏体组织.

参考文献:

[1] 刘　健,王树奇,李志忠,等. 接地网腐蚀故障诊断的可测性研究[J]. 高电压技术,2008,34(1): 64 - 69.
Liu Jian, Wang Shuqi, Li Zhizhong, *et al*. Testability of grounding grids corrosion diagnosis [J]. High Voltage Engineering, 2008, 34(1): 64 - 69.

[2] 陆培钧,黄松波,豆　朋,等. 佛山地区变电站接地网腐蚀状况分析[J]. 高电压技术,2008,34(9): 1996 - 1999.
Lu Peijun, Huang Songbo, Dou Peng, *et al*. Corrosion analysis on earthing network of foshan substation [J]. High Voltage Engineering, 2008, 34(9): 1996 - 1999.

[3] 张秀丽,骆　平,莫　逆,等. 接地网腐蚀状态电化学检测系统的开发与应用[J]. 中国机电工程学报,2008,28(19): 152 - 156.
Zhang Xiuli, Luo Ping, Mo Ni, *et al*. Development and application of electrochemical detection system for grounding grid corrosion state [J]. Proceedings of the CSEE, 2008, 28(19): 152 - 156.

[4] 郑敏聪. 杂散电流对变电站接地网材料耐蚀性的影响[J]. 腐蚀与防护,2010,31(4): 294 - 296.
Zheng Mincong. Effect of stray current on corrosion resistance of grounding grid materials at substation [J]. Corrosion & Protection, 2010, 31(4): 294 - 296.

[5] 谭建红,张胜涛,曹阿林,等. 土壤环境中钢的杂散电流腐蚀研究[J]. 材料导报,2011,25(2): 107 - 111.
Tan Jianhong, Zhang Shengtao, Cao Alin, *et al*. Stray current corrosion behavior of steel in soil environments [J]. Materials Review, 2011, 25(2): 107 - 111.

[6] 周贤良,李晖榕,华小珍,等. X80 管线钢埋弧焊焊接接头的组织和腐蚀性能[J]. 焊接学报,2011,32(1): 37 - 40.
Zhou Xianliang, Li Huirong, Hua Xiaozhen, *et al*. Microstructures and corrosion properties of submerged arc welded joint for X80 pipeline steel [J]. Transactions of the China Welding Institution, 2011, 32(1): 37 - 40.

[7] 曹楚南,常晓元,林海潮. 孔蚀过程的电化学噪声特征[J]. 中国腐蚀与防护学报,1989,9(1): 21 - 27.
Cao Chunan, Chang Xiaoyuan, Lin Haichao. Features of electrochemical noises during pitting corrosion [J]. Journal of Chinese

Society for Corrosion and protection, 1989, 9(1): 21 – 27.

[8] 黄家怿，邱于兵，郭兴蓬. 采用聚类分析研究X70钢在库尔勒土壤中初期电化学噪声特征 [J]. 中国腐蚀与防护学报，2009，29(6)：453 – 458.
Huang Jiayi, Qiu Yubing, Guo Xingpeng. Cluster analysis of electrochemical noise for X7o steel in kuerle soil [J]. Journal of Chinese Society for Corrosion and protection, 2009, 29(6): 453 – 458.

[9] 董泽华，郭兴蓬，郑家燊. 电化学噪声的分析方法 [J]. 材料保护，2001，34(7)：20 – 23.
Dong Zehua, Guo Xingpeng, Zheng Jiashen. Review on electrochemical noise analysis methods [J]. Materials Protection, 2001, 34(7): 20 – 23.

[10] 张鉴清，张 昭，王建明，等. 电化学噪声的分析与应用—Ⅰ. 电化学噪声的分析原理 [J]. 中国腐蚀与防护学报，2001，21(5)：310 – 320.
Zhang Jianqing, Zhang Zhao, Wang Jianming, *et al*. Analysis and application of electrochemical noise I. theory of electrochemical noise analysis [J]. Journal of Chinese Society for Corrosion and protection, 2001, 21(5): 310 – 320.

[11] Eden D A, John D G, Dawson J L. Comparison of electrochemical potential noise to the electrochemical current noise to provide a resistive noise which is inversely proportional to the corrosion current: United States, US5139627 A [P]. 1992 – 08 – 18.

[12] 曹楚南. 腐蚀电化学原理 [M]. 北京：化学工业出版社，2004.

[13] Eden D A, Rothwell A N. Electrochemical noise data: analysis interpretation and presentation [C] // Corrosion, National Association of Corrosion Engineers, Houston, 1992: 1 – 8.

[14] Gouveia C C, Pereira M I S, Brett C M A. Electrochemical noise and impedance study of aluminium in weakly acid chloride solution [J]. Electrochemical Acta, 2004, 49(5): 785 – 793.

[15] Chen J F, Bogaerts W F. The physical meaning of noise resistance [J]. Corrosion Science, 1995, 37(11): 1839 – 1842.

[16] 孔小东，杨明波，朱梅五. 冶金因素对低合金钢焊接接头耐蚀性的影响 [J]. 焊接学报，2009，30(7)：105 – 109.
Kong Xiaodong, Yang Mingbo, Zhu Meiwu. Effects of metallurgical factors on corrosion behaviors of welded joints of low-alloy steels [J]. Transactions of the China welding Institution, 2009, 30(7): 105 – 109.

[17] 雷阿利，冯拉俊，张 敏，等. 不同方法焊接的Q235钢接头在亚铵介质中耐蚀性分析 [J]. 焊接学报，2007，28(8)：65 – 68.
Lei Ali, Feng Lajun, Zhang Min, *et al*. Corrosion behavior of Q235 steel joint welded by different methods in the ammonium sulfite [J]. Transactions of the China Welding Institution, 2007, 28(8): 65 – 68.

作者简介： 冯拉俊，男，1957年出生，博士，教授，博士研究生导师. 主要从事材料的腐蚀与防护方面的科研及教学工作. 发表论文90余篇. Email: fenglajun@xaut.edu.cn

[上接第68页]

[4] 王 威，徐广印，王旭友，等. 1420铝锂合金激光焊接气孔抑制技术 [J]. 焊接学报，2008，29(2)：5 – 7.
Wang Wei, Xu Guangyin, Wang Xuyou, *et al*. Porosity prevention of 1420 Al-Li alloy for laser welding [J]. Transactions of the China Welding Institution, 2008, 29(2): 5 – 7.

[5] Susumu T, Isao K, Gori A. Suppression of welding defects in deep penetration CO_2 laser welding [C] // International Congress on Applications of Lasers & Electro-Optics, Dearborn, 2000: 7 – 15.

[6] 赵 琳，张旭东，陈武柱，等. 光束摆动法减小激光焊接气孔倾向 [J]. 焊接学报，2004，25(1)：29 – 32.
Zhao Lin, Zhang Xudong, Chen Wuzhu, *et al*. Repression of porosity with beam weaving laser welding [J]. Transactions of the China Welding Institution, 2004, 25(1): 29 – 32.

[7] 包 刚，彭 云，陈武柱，等. 超细晶粒钢光束摆动激光焊接的研究 [J]. 应用激光，2002，22(2)：203 – 205.
Bao Gang, Peng Yun, Chen Wuzhu, *et al*. Study on laser welding of ultra-fine grained steel with weaving beam [J]. Applied Laser, 2002, 22(2): 203 – 205.

[8] Zhang X D, Chen W Z. Improvement of weld quality using a weaving beam in laser welding [J]. Journal of Materials Science & Technology, 2004, 20(5): 633 – 636.

作者简介： 周立涛，男，1988年出生，硕士. 主要从事高强铝合金、钛合金激光焊接和激光扫描焊接方面的研究工作. 发表论文2篇. Email: zlt88510@163.com

通讯作者： 王旭友，男，研究员. Email: 13115600580@163.com

Microstructure and wear resistance of laser amorphous-nanocrystals reinforced Ni-based coating on TA15 titanium alloy LI Jianing[1,2], GONG Shuili[1], LI Huaixue[1], SHAN Feihu[1] (1. Science and Technology on Power Beam Processes Laboratory, Beijing Aeronautical Manufacturing Technology Research Institute, Beijing 100024, China; 2. Aviation Industry Corporation of China, Beijing Institute of Aeronautical Materials, Beijing 100095, China). pp 57 - 60

Abstract: Coaxial powder feeding laser cladding of the Ni60A-Ni coated WC-TiB_2-Y_2O_3 mixed powders on the aviation material TA15 titanium alloy substrate can form an amorphous-nanocrystals reinforced composite coating. Such coating was researched by means of the microstructure observation, the microhardness test and the dry friction and wear test at room temperature. Investigation indicated that the such coating mainly consisted of γ-(Fe, Ni), WC, α-W_2C, $M_{12}C$, Ti-B compounds, Ti-Al intermetallics, amorphous phases and the Mo, Zr, V carbides. Amorphous, nanocrystalline and the other crystalline phases were existence in such coating. This coating also exhibited a better wear resistance than TA15 titanium alloy, and abrasive grain wear mechanism and the adhere wear mechanism did the process at the same time during the dry sliding wear process. The productions of the nanocrystals made the worn surface more smooth, favoring the decrease of the coefficient of friction and the wear volume losses.

Key words: laser cladding; surface modifications; wear properties

Weld defect detection by X-ray images method based on Fourier fitting surface LI Xueqin[1], LIU Peiyong[2], YIN Guofu[2], JIANG Honghai[3] (1. School of Mechanical Engineering and Automation, Xihua University, Chengdu 610039, China; 2. School of Manufacturing Science and Engineering, Sichuan University, Chengdu 610065, China; 3. School of Electrical and Mechanical Engineering, Kunming University of Science and Technology, Kunming 650504, China). pp 61 - 64

Abstract: To solve such problems as the strong noise, low contrast and complex background of X-ray image in the weld defect detection, a method of the noise reduction, weld edge segmentation and defects extraction was proposed. The fast discrete curvelet transform and cycle shift were applied to reduce noise of the weld image, and the Otsu method was utilized to extract the weld region by the column gray curves of the image. Cubic Fourier curve was used to fit the column gray curves after preprocessing of weld image, and the adaptive threshold surface was constructed by extending fitting curves to 3D space. Finally, the background and the defect area were segmented accurately with the gray differences of 3D gray image between the original image and the reconstructed surface. Experiment results show that the method can extract weld defects accurately. Compared with traditional defect detection algorithm, it has the lower undetected rate and fewer misinterpretations, the accuracy rate could reach 95%.

Key words: X-ray; weld image; defect detection; curvelet transform; Fourier fitting

Effects of laser scanning welding process on porosity rate of aluminum alloy ZHOU Litao, WANG Wei, WANG Xuyou, WANG Shiyang, SUN Qian (Harbin Welding Institute, China Academy of Machinery Science and Technology, Harbin 150028, China). pp 65 - 68, 72

Abstract: Research of 6061 aluminum alloy was done by using laser-scanning welding. The effects of such scanning parameters as track, width and frequency on porosity tendency were studied. The result showed that laser-scanning welding with the path of vertical, parallel and circular to welds can reduce the porosity of aluminum alloy compared with laser welding without scanning and the circular pattern was the best. The scanning width and scanning frequency of laser also have important influence on porosity, which can be controlled within 0.5% as the scanning width was greater than 0.65 mm and scanning frequency was from 100 to 220 Hz. The producing of porosity was associated with weld shape and the lower of depth-to-width ratio of the weld can help to control the porosity.

Key words: aluminum alloy; laser scanning welding; porosity inhibition

Corrosion behavior of weld joints of substation grounding grid FENG Lajun[1], DENG Bo[1], YAN Aijun[2], ZHANG Jing[1] (1. Material Corrosion and Protection Key Laboratory of Xi'an, Xi'an University of Technology, Xi'an 710048, China; 2. Shaanxi Electric Power Research Institute, Xi'an 710054, China). pp 69 - 72

Abstract: To provide foundation for corrosion protection of the weld metal using in grounding grid, the corrosion difference between the weld and base metal of grounding grid was studied by electrochemical noise and field coupon method. The results showd that there were many transients in the time series of the weld of Q235 steel for grounding grid in soil of Shaanxi Xiaoyi substation, while a few transients in the time series of the Q235 base metal, which indicated that weld corrosion was more sensitive to discharge voltage of grounding grid. The noise resistance of the weld metal, Rn, was 3.38×10^4 Ω/cm^2 during the corrosion process, and the Rn of the weld was 1.44×10^4 Ω/cm^2. The corrosion rate of the weld metal was 0.067 mm/a, and for the welded joint was 0.077 mm/a. The based metal was in a uniform type of corrosion and the weld was mainly in a pitting type of corrosion.

Key words: grounding grid; weld corrosion; electrochemical noise; localized corrosion

Research on toughness weak points of joints of NiCrMoV refractory steel for manufacturing steam turbine rotor LI Yifei[1], CAI Zhipeng[1], PAN Jiluan[1], LIU Xia[1,2], WANG Peng[2], HUO Xin[2], SHEN Hongwei[2] (1. Department of Mechanical Engineering, Tsinghua University, Beijing 100084, China; 2. Shanghai Electric Power Generation Equipment Co. Ltd., Shanghai 200240, China). pp 73 - 76, 80

Abstract: The toughness weak points of multi-layer and multi-pass weld of 30Cr2Ni4MoV refractory steel steam turbine welded rotor were studied by means of simulated heat welded layers with the emphasis on the forming of the toughness weak points and its influence on the toughness. The methods of optical microscope analysis, scanning electron microscopy analysis and transmission electron microscope analysis were utilized. The experimental results show that there are many M-A constituents in the carbon-rich areas of welded layers, which is disadvantageous to the toughness. The influence of the M-A constituents on the weld